



1 **Spatial and temporal simulation of groundwater recharge and cross-**
2 **validation with point measurements in volcanic aquifers with variable**
3 **topography**

4 Alemu Yenehun^{a,b}, Mekete Dessie^c, Fenta Nigate^a, Ashebir Sewale Belay^{a,b}, Mulugeta Azeze^c, Marc Van Camp^b,
5 Derbew Fenetie Taye^f, Desale Kidane^{e,f}, Enyew Adgo^f, Jan Nyssen^g, Ann van Griensven^d, Kristine Walraevens^b

6 ^a*School of Earth Sciences, Bahir Dar University, Bahir Dar, Ethiopia*

7 ^b*Laboratory for Applied Geology and Hydrogeology, Department of Geology, Ghent University, Ghent, Belgium*

8 ^c*Faculty of Civil and Water Resources Engineering, Bahir Dar University, Bahir Dar, Ethiopia*

9 ^d*Department of Hydrology and Hydraulic Engineering, Vrije Universiteit Brussel, Brussel, Belgium*

10 ^e*Department of Soil Physics, Ghent University, Belgium*

11 ^f*Department of Natural Resources, Bahir Dar University, Ethiopia*

12 ^g*Department of Geography, Ghent University, Belgium*

13 Correspondence to: Alemu Yenehun (abrexyene@email.com)

14 ***Abstract***






15 A physically distributed water balance model called WetSpass is applied to estimate the
16 recharge for the semi-humid Lake Tana basin in northwest Ethiopia. Lake Tana basin is one of the
17 growth corridors of the country, where huge waterworks infrastructure is developing. Estimating
18 groundwater recharge at required spatial and temporal scales is a challenge in groundwater
19 management, sustainability and pollution studies. In this study, the WetSpass model is developed
20 at 90 m grid resolution. The spatial recharge map by WetSpass is cross-validated with water table
21 fluctuation (WTF) and chloride mass balance (CMB) methods. The mean annual recharge, surface
22 runoff, and evapotranspiration over the whole basin using WetSpass are estimated at 315 mm, 416
23 mm, and 770 mm of rainfall, respectively. The mean annual recharge ranges from 0 mm to 1085
24 mm (0% to 57% of the rainfall): 0 mm at water bodies and highest on flat, sandy loam soil and
25 bush land cover. Similarly, a high range of recharge is also noted using WTF and CMB methods
26 showing the strong heterogeneous nature of the hydro(meteoro)logical characteristics of the area.
27 Generally, the recharge is found higher in southern and eastern catchments and lower in the
28 northern catchments, primarily due to higher rainfall amounts in the former parts. A fair general
29 correlation between the recharge by WTF and WetSpass is found. WetSpass is effective in aquifers
30 where diffuse recharging mechanism is the predominant type and recharge is controlled by rainfall.



31 It is less effective in the storage-controlled flat floodplain alluvial and fractured rock aquifer areas.
32 In these areas, the point estimates by WTF and CMB are effective and can be considered as reliable
33 values. The land use change from 1986 to 2014 brought a relatively small hydrological change in
34 recharge although the land use has changed significantly.

35 **Keywords: Lake Tana basin; recharge; WetSpa; WTF; CMB; storage controlled; diffuse**
36 **recharge**

37 1. Introduction

38 Groundwater recharge is all water that reaches the groundwater aquifer from any direction
39 (Scanlon et al., 2002). In specific terms, it is defined as the height of the water column that enters
40 the groundwater  after crossing the vadose zone in a specific period (Manna et al., 2016).
41 Understanding recharge processes and its quantification is vital for proper management and
42 protection of the lim  groundwater resources (Ferede et al., 2020; Healy and Cook, 2002;
43 Uugulu and Wanke, 2020). However, it is one of the most difficult water balanc  components to
44 be evaluated with acceptable accuracy (Hornero et al., 2016). This is particularly true in areas with
45 wide heterogeneity of geological, topographical, and hydro-climatic conditions. Thus,
46 groundwater  management and development policymakers and practitioners should take
47 recharge estimations and their uncertainty into account in the management plans (Hornero et al.,
48 2016). As recharge processes significantly vary from area to area, there is no guarantee that one
49 method effectively used for one locality will give reasonable results when applied for another 
50 (Obuobie et al., 2012). Different methods are developed for recharge estimation. However,
51 choosing appropriate methods is often challenging. Important considerations in choosing a
52 technique include space/time scales, range, and reliability of recharge estimates which in turn
53 depend on the goal of the study (Scanlon et al., 2002). For instance, groundwater resources
54 assessment of an area may be achieved at a small space/time scale but flow and contaminant
55 modeling need quantification of recharge amounts at large spatial as well as temporal scales.

56 There is a strong groundwater recharge variability across the Ethiopian volcanic rock aquifers
57 (Alemayehu and Kebede, 2011; Ayenew et al., 2008; Demlie et al., 2008, 2007b; Kebede et al.,
58 2005). Lake Tana basin, which is one of the major basins in the Ethiopian volcanic plateau, has
59 high hydrogeological and topographical variabilities. Furthermore, the area has a climate with long



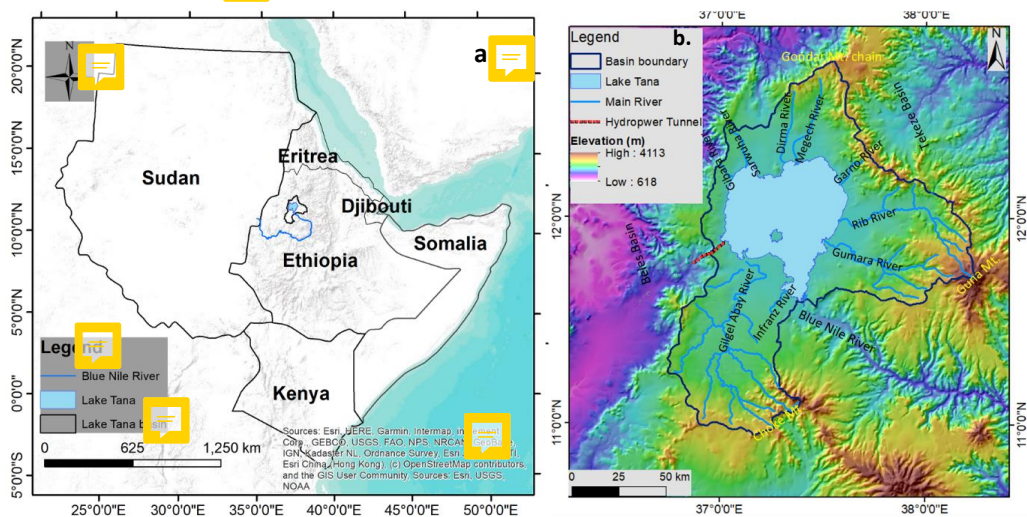
60 dry winters and short rainy summer seasons. Hence, the groundwater recharge-discharge processes
61 are expected to vary highly both spatially and temporal. There are a number of recharge
62 estimation methods whose effectiveness depend on the recharge mechanism (Healy and Cook,
63 2002). Hence, understanding and identifying the recharging mechanism of aquifers and the
64 assumptions of different estimations methods is a key to effectively choose among the different
65 techniques (Scanlon et al., 2002; Tilahun et al., 2009). On fractured aquifers where preferential
66 flow dominates, focused recharge is a major recharge mechanism rather than the diffuse recharge.
67 Water balance models estimate better the diffuse recharge (Zhu et al., 2020), while water point
68 measuring-based methods such as water table fluctuation are preferable for focused recharge
69 mechanisms (Scanlon et al., 2002). One of the challenges for the point recharge estimation
70 methods is their incapability to estimate it in a spatially distributed way. Given the high spatial
71 variability of recharge, due to variations in geology, topography, soil texture, land use, and
72 meteorological variables, it is unwise to extrapolate or regionalized the result by the conventional
73 point recharge estimation techniques (Tilahun and Merkel, 2009). Hence, in this study, a
74 physically-based water balance model called WetSpass, which simulates recharge in a spatially
75 and temporally distributed manner is applied. Water table fluctuation and chloride mass balance
76 methods have been used to identify the recharge mechanisms, to compare and cross-validate the
77 results with the WetSpass model. These methods have been applied in several studies: the WetSpass
78 model for example in Batelaan and De Smedt (2007, 2001), Gebreyohannes et al. (2013), Graf and
79 Przybyłek (2018), Salem et al. (2019), Ashaolu (2020), Yenehun et al. (2020); the WTF method
80 for example in Sophocleous (1991), Healy and Cook (2002), Moon et al. (2004), Crosbie et al.
81 (2005), Chal et al. (2006), Mikunthan and De Silva (2009), Nigate et al. (2020), Yenehun et al.
82 (2020); and the CM method for example in Allison and Hughes (1978), Allison (1988), Guan et
83 al. (2010), Somaratne and Smettem (2014), Uugulu and Wanke (2020), Yenehun et al. (2020).

84 The main objectives of this study are: 1) to determine groundwater recharge of the Lake Tana
85 basin in a spatially distributed way; 2) to identify controlling factors for the spatial variability of
86 the recharge in the basin; 3) to compare and evaluate the recharge estimation methods over the
87 basin; 4) to evaluate the effect of land use change over the hydrology of Lake Tana basin, and 5)
88 to determine the spatial and seasonal variation of runoff and evapotranspiration in the basin.



89 2. Study area location, geology, and hydrogeology

90 The Lake Tana Basin (Fig. 1) consists of the Lake Tana water body which is the largest natural
91 lake in Ethiopia. It is the source and head of the upper Blue Nile Basin which is the major tributary
92 to the Nile Basin. The Nile Basin is shared by eleven riparian countries and is the lifeline for more
93 than 238 million people living in the basin (Dile et al., 2018; Tekleab et al., 2011). Lake Tana
94 Basin has a total drainage area of approximately 15,077 km², of which the lake covers about 3,077
95 km². It is a shallow lake, which is situated in the northwestern Ethiopian highlands and receives
96 flow from more than 40 rivers (Dessie et al., 2015, 2014; Rientjes et al., 2011; Wale et al., 2009).

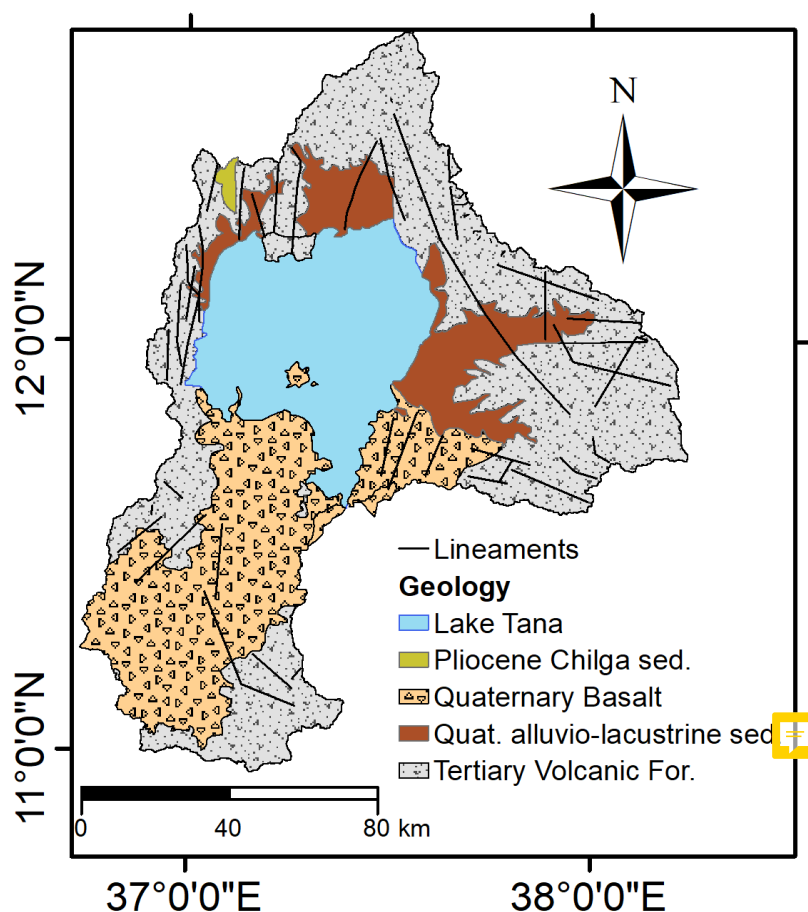


97
98 Fig. 1. Location map of Lake Tana basin showing the location of the Lake Tana basin within Ethiopia
99 and its neighbors (a), and topographical setup and main rivers (b). The Blue Nile, and the
100 Tekeze basins are the major adjacent basins for Lake Tana Basin.

101 The Lake Tana basin is perched on a topographic dome, which is within an overall configuration
102 of an uplifted dome that was active during the Tertiary volcanic events. The Lake Tana basin was
103 formed by the junction of three grabens (Chorowicz et al., 1998). It acquired its present form
104 through damming by Quaternary lava flow aged to 10,000 years on its southern part (Jepsen and
105 Athearn, 1961). Stratified Tertiary volcanic rock piles in northwestern Ethiopia overlie Mesozoic
106 sedimentary rock stratigraphical sequence (Chorowicz et al., 1998). They have an average
107 thickness of 1 to 1.5 km (Jepsen and Athearn, 1961; Minucci, 1938), and covers a significant area
108 of the basin (Fig. 2). Quaternary basalt covers most of the southern part of the Tana Basin (Jepsen



109 and Athearn, 1961). Sedimentary deposits such as the Pliocene Chilga sediment and recent alluvio-
110 lacustrine sediments on the extensive floodplains of the northern and eastern catchments are also
111 among major lithological coverages (Fig. 2).



112
113 *Fig. 2. Geological map of Lake Tana basin modified after Nigate (2019)*

114 The complex nature of the aquifers, owing mainly to multi-stage volcanism at different
115 volcanic centers, and hence the presence of different volcanic rock types (with complex
116 geometrical setting) in the Ethiopian volcanic plateau, has led to a strong spatial groundwater
117 potential and recharge variability (Alemayehu and Kebede, 2011; Ayenew et al., 2008; Demlie et
118 al., 2008, 2007b; Kebede et al., 2005). The water level for aquifers lying at different physiography
119 in the highlands of the Lake Tana basin responds differently to the rainfall and has a different
120 recharging mechanism (Yenehun et al., 2020).



121 3. Data and methods

122 3.1. WetSpa model

123 For this study, the WetSpa model written in Python (WetSpa-M) is applied. The WetSpa
124 (an acronym for Water and Energy Transfer in Soil, Plants, and Atmosphere under quasi Steady
125 State) was first developed by Batelaan and De Smedt (2001) and later modified by Batelaan and
126 De Smedt (2007). It is a numerical model to simulate long-term average spatial distributions of
127 hydrological parameters and processes at a basin-scale in quasi-steady state. It means the model is
128 restricted to temporal variations only at the seasonal or monthly time scale. That means years of
129 seasonal or monthly time series data are averaged into single seasons or months. The model
130 subdivides the precipitation into the runoff (to refer only to surface component of the river flow in
131 this paper), evapotranspiration, and groundwater recharge, and estimates long-term seasonal
132 values as distributed spatial maps.

$$133 \quad P = S + ET + R \quad (1)$$

134 Where P is precipitation [L], S is runoff [L], ET is evapotranspiration [L], and R is groundwater
135 recharge [L].

$$136 \quad S = f_1 * P_n \quad (2)$$

137 Where f_1 is a runoff factor that depends on land use and vegetation characteristics, soil texture,
138 and slope. P_n is the net precipitation reaching the ground surface (total precipitation minus
139 interception by the plant canopy).

$$140 \quad ET = f_2 * EP \quad (3)$$

141 Where f_2 is an evapotranspiration factor which depends on land use and vegetation characteristics
142 and soil texture, and EP is the potential evaporation of open water [L].

143 Groundwater recharge is estimated as the closure term of equation 1.

144 The WetSpa-M model calculates each hydrological term at pixel scale by subdividing each
145 pixel into open water, impervious surface area, bare soil, and vegetated area. Percentage values of
146 these subdivisions of a pixel are assigned for all possible land use classes in the parameter table of
147 the model. However, some percentage values have been modified based on local expert judgment.



148 In this study, the model is developed at 90 m x 90 m grid resolution. Hence, all the input
149 parameter grid maps are resampled to the same grid size. The model area is equally meshed and
150 has 1824 columns and 2223 rows. WetSpass has parameter tables as an input besides the grid
151 maps. Some land-use parameter values and the number of rainy days are modified into local
152 contexts based on measured data and our expert knowledge whereas the default values of soil-
153 related parameters have been kept. For example, the root depth for forest land use is changed from
154 2 m to 5.5 m, because eucalyptus (the dominant forest tree in the area) is deep-rooted. A similar
155 modification was made by Yenehun et al. (2020) for the highland part of the Gilgel Abay
156 catchment.

157 The developed WetSpass model is calibrated manually by adjusting the global model
158 parameters, such as rainfall intensity, soil moisture alfa coefficient (α), LPa calibration parameter
159 for adjusting the potential evapotranspiration depending on the soil moisture, interception
160 parameter (a), and runoff delay factor (x). In the calibration process, the goodness of fit between
161 the simulated and measured runoff for major rivers was being checked and has been used for
162 further model optimization. Furthermore, the point recharge values determined by the WTF
163 method and extracted recharge of the WetSpass spatial map are compared, thereby validating the
164 result.

165 For model calibration, the recent land use (land use 2014) (Fig. 4c) has been used. After the
166 model is calibrated to the optimal possible using this land use, the model is run for land uses 1986
167 and 2000 (Figs. 4a and b). Hence, the effect of land use change on the seasonal water balance terms
168 has been evaluated.

169 3.1.1. Data for WetSpass model

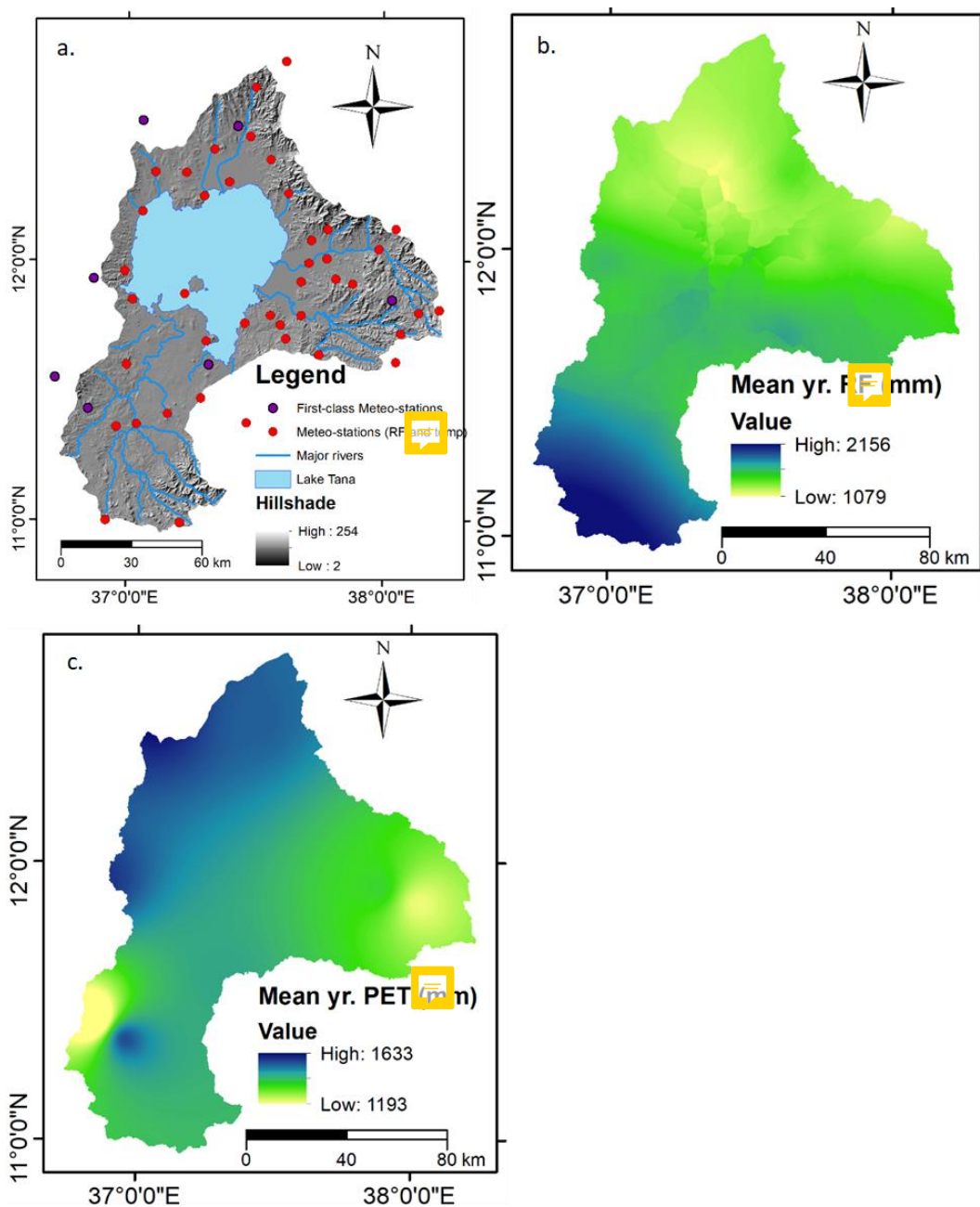
170 Meteorological data consisting of rainfall, temperature (minimum, maximum, average),
171 relative humidity, sunshine hours, and wind speed, and GIS spatial maps including land use, soil
172 texture, elevation, slope angle, and groundwater level have been used for the WetSpass model.
173 The meteorological data were collected from the Ethiopian National Meteorological Agency
174 (NMA Bahir Dar branch, and our simple meteorological stations (measuring only rainfall and
175 temperature). The WetSpass model uses the long-term average raster grid maps of rainfall,
176 potential evapotranspiration (PET), mean temperature, and wind speed (Batelaan and De Smedt,
177 2007, 2001). The WetSpass model calculates the water balance of an area at a relatively coarse



178 time scale (per month to the finest). However, for semi-humid tropical regions where most of the
179 months are dry winter, applying the model at the seasonal time scale is preferable. Hence,
180 preparation of these data for summer and winter is done. The wet summer consists of months from
181 June to September and the dry winter from October to May. Gebreyohannes et al. (2013) worked
182 similarly for their application of the method at the Geba catchment in northern Ethiopia.

183 The long-term seasonal average point rainfall depth (mostly from 2005 to 2018) is prepared
184 from 50 meteorological stations distributed mainly from the basin and a few from the surroundings
185 (Fig. 3a). 42 of the stations were from NMA, and the remaining 8 were our own. The data from
186 our stations were short-term ones, comprising only 2017 to 2019. The areal rainfall depth maps
187 for both summer and winter are produced through the kriging interpolation since the number of
188 input stations was relatively high and appropriate for this interpolation technique. Mean annual
189 temperature raster maps for both the summer and winter seasons are prepared from 30 stations
190 using the inverse distance weighting (IDW) method. Similarly, IDW is applied for windspeed
191 using data from only 7 so-called first-class meteorological stations (Fig. 3a).

192 For the potential evapotranspiration, the Penman-Monteith method, modified by Allen et
193 al. (1998), is applied to calculate point PET values at 8 stations (Fig. 3a). For the spatial
194 interpolation IDW is applied and maps for both summer and winter are produced. The mean annual
195 PET map is presented in Fig. 3. The groundwater depth grid map is needed in the WetSpass model
196 primarily to calculate evapotranspiration from the groundwater, and for delineation of wetlands,
197 so that water balance calculations include seepage fluxes (Batelaan and De Smedt, 2007;
198 Gebreyohannes et al., 2013). Hence, the groundwater level grid maps for both summer and winter
199 seasons are prepared using time series groundwater level data collected for this study. First, an
200 average depth to water table raster map by classifying the area into high middle and low elevations
201 is prepared using our groundwater monitoring points. Then this raster map consisting of three
202 different depth to water table raster values is subtracted from the DEM of the area to obtain the
203 hydraulic head raster ASCII map which is the input of the WetSpass model. A similar method is
204 followed for both summer and winter. Furthermore, the WetSpass model is calibrated using river
205 flow data measured at different major rivers of the basin. Hence, mean annual river discharge data
206 measured by Dessie et al. (2015) in the years 2012-2015 have been taken.



207

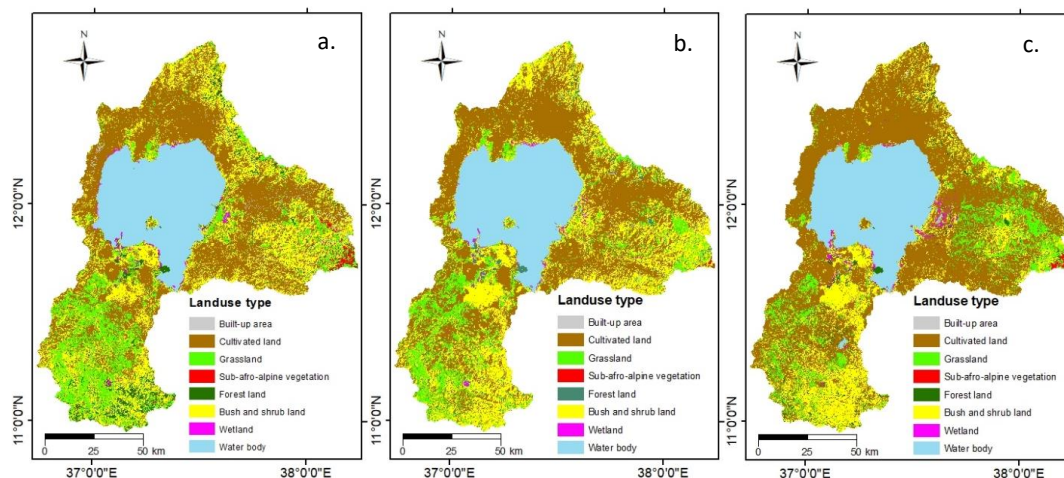
208 Fig. 3. (a) There are a total of 50 meteorological stations among which eight stations are measuring
209 minimum and maximum temperatures, rainfall, windspeed, relative humidity, and sunshine hours. (b)
210 mean annual rainfall map is produced by Kriging interpolation using data from the 50 meteorological



211 stations. (c) The long-term mean annual PET map is produced through IDW interpolation from the
212 first-class meteorological stations. The point PET data were calculated by the Penman-Monteith method.

213 The rainfall has high spatial variation, with minimum and maximum mean annual of 1079
214 mm and 2156 mm, respectively (with a standard deviation of 216). The rainfall is generally higher
215 in the southern, and lower in the northern parts of the study basin (Fig.3b). The lower recorded
216 in the flat floodplain of the northern (Megech) catchment, and highest at the southern highlands
217 (Figs. 1 and 3a, 3b). There is a poor correlation between rainfall and topographical elevation,
218 similar to what was reported by Dessie et al. (2014). The maximum and minimum potential
219 evapotranspiration are 1633 mm and 1193 mm, respectively, with a mean of 1478 mm and a
220 standard deviation of 70. The higher values on the northwestern, and lower towards the south and
221 eastern highlands (Fig. 3c). There is generally a good correlation between elevation and PET
222 values. The relatively few numbers of meteorological stations for PET interpolation is one of the
223 limiting factors in this study.

224 GIS spatial maps are taken from different sources and adapted according to the model
225 requirement of the WetSpss model. The historical land use maps were prepared by the Amhara
226 Design and Supervision Water Works Enterprise (ADSWE) (ADSWE, 2015a). They prepared
227 land use maps for the years 1986, 2000, and 2014 using satellite images (SPOT and Landsat) and
228 Google Earth, as well as ground-truthing. Each land use type coverage and change of the
229 classification periods are presented (Table 4). The coding number assigned for land use types in
230 the WetSpss model is given for each class so that the model can read and related with land use
231 parameter table. Appropriate correspondence between the local land use classes and the model
232 parameter tables has been made.



233

234 Fig. 4. Land use map of 1986 (a), 2000 (b), and 2014 (c) prepared by the Amhara D
 235 Water Works Enterprise.

236 Table 1. Classified land use types areal coverage in km² and percentage of each cover type to the total are
 237 Tana basin at different years.



Cover type	Area coverage (in km ²) in the classification years and % of each class					
	1986	%	2000	%	2014	%
Built-up area	148.7	1	42.8	0.3	43.6	0.3
Cultivated land	5,530.2	36.7	6,151.9	40.8	7,383.6	49
Grass land	1,822.2	12.1	1,575.9	10.5	1,434.6	9.5
Sub-afro-alpine vegetation	122	0.8	10.6	0.1	38.2	0.3
Forest land	656.8	4.4	349.2	2.3	271.6	1.8
Bush and shrub land	3,640	24.1	3,784.7	25.1	2,688.1	17.8
Wetland	107.1	0.7	100.2	0.7	118.2	0.8
Water body	3,051.2	20.2	3,062.9	20.3	3,100.4	20.6
Total	15,078	100	15,078	100	15,078.2	100



238

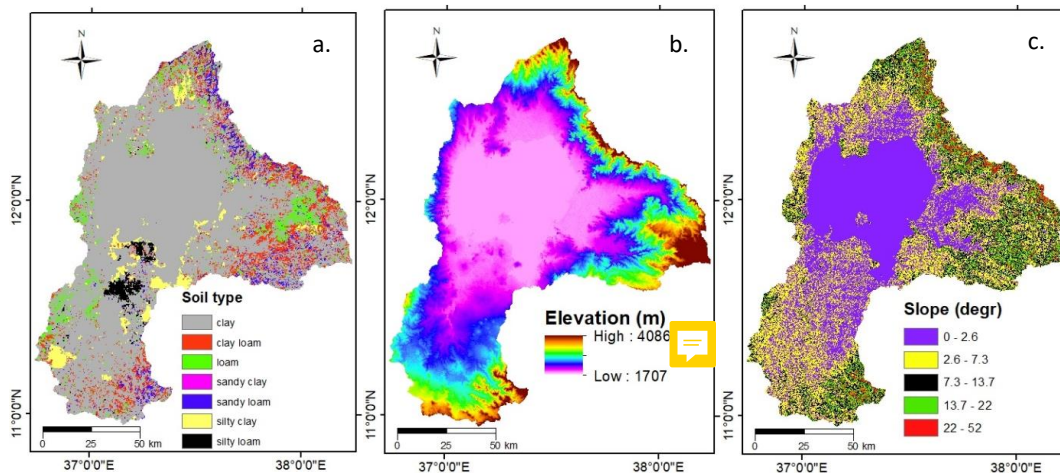
239


The soil map of the Tana basin used for the modeling is prepared by ADSWE (ADSWE, 2015b). It was prepared through a detailed field survey, sampling, and analysis aided by satellite



240 image information. The soils of the basin were identified and classified based on soil genesis,
241 morphological and surface characteristics according to FAO (1998, 2006) soil map of the world.
242 The results of this soil resource assessment reveal that twelve major agricultural soil types are
243 present in the study area. However, WetSpss needs textural soil classes. Textural  classes have
244 been given for most of the 101 mapping units. But for a few of the mapping pixels, the textural
245 class column was found blank in the attribute table of the soil map, and thus we have filled it based
246 on the association of major soil type and common texture in the other mapping units. We have also
247 used our expertise area knowledge in filling th  gaps. Finally, codes for each of the seven textural
248 soil classes (Fig. 5a) are assigned, as per in the WetSpss model.

249 A digital elevation model (DEM) with 20 m resolution is found from the Global Land
250 Cover Facility (rsdac.jspacesystems.or.jp/">http://glo  rsdac.jspacesystems.or.jp/). After filling the possible holes,
251 resampling to 90 m was done and the final raster map for elevation has been prepared (Fig. 5b).
252 Similarly, the slope an  is extracted in ArcGIS 10.3 from the DEM and resampled to 90 m
253 resolution (Fig. 5c).



254
255 *Fig. 5. The soil (a), the ele  n (b), and the slope angle (c) spatial maps of the Lake Tana basin*
256 *with a resolution of 90 m*



257 3.2. Water table fluctuation (WTF) and Chloride mass balance (CMB) 258 methods

259 The WTF method is among the most widely used techniques for groundwater estimation of
260 aquifers (Healy and Cook, 2002). The method has been applied in many studies (e.g., Sophocleous,
261 1991; Healy and Cook, 2002; Moon et al., 2004; Crosbie et al., 2005; Chal et al., 2006; Mikunthan
262 and De Silva, 2009, Yenehun et al., 2020). The method uses the following formula to calculate
263 recharge:

$$264 \text{ Recharge} = S_y \frac{\Delta h}{\Delta t} \quad (4)$$

265 where Δh is the head change comparing before and after the rainfall season, S_y is the specific
266 yield, and Δt is the time interval for the recharge period.

267 According to Delin et al. (2007) and Healy and Cook (2002), for the application of the WTF
268 method, the following assumptions should be satisfied: 1) sharp water level rises and declines in
269 response to only groundwater recharge and discharge; 2) the aquifer system needs to be unconfined
270 with shallow water level; S_y the specific yield should be known and constant. Hence, the
271 monitoring well hydrographs are evaluated, and only those which are more or less in line with
272 these assumptions are considered for the point recharge calculation of this study. Similar to the
273 suggestion of Healy and Cook (2002), the graphical method is applied to extrapolate the recession
274 of the pre-recharge water level to the recharge period so that the water level fluctuation is
275 accurately considered. The main source of uncertainty for the application of the method is the
276 possible errors in the estimation of the specific yield (Healy and Cook, 2002; Yenehun et al., 2020).
277 In this study, both literature from Johnson (1967), and an empirical formula developed by Beretta
278 and Stevenazzi (2018) have been applied. Beretta and Stevenazzi (2018) developed a relationship
279 between S_y and hydraulic conductivity (k). Hence, using the formula, S_y values for monitoring
280 wells were determined using the k values analyzed from our single well pumping and slug test
281 results.

282 Similar to WTF, the chloride mass balance (CMB) method is a widely applied technique for
283 estimating recharge (Somaratne and Smettem, 2014). The main concept in the method is that the
284 increase in the concentration of chloride in the groundwater compared to the rainwater is due to
285 evapotranspiration in the vadose zone during infiltrating/percolating (Allison and Hughes, 1978;



286 Allison, 1988; Guan et al., 2010; Somaratne and Smettem, 2014). It means chloride anion is a
287 conservative ion and its concentration increment during its movement in the vadose zone is merely
288 in response to evapotranspiration. Mathematically, groundwater recharge (GWR) is calculated in
289 the following way:

$$290 \quad GWR = Pe * \frac{Cl_p}{Cl_{gw}} \quad (5)$$

291 Where GWR is groundwater recharge, Cl_p is chloride concentration in precipitation, Cl_{gw} is
292 chloride concentration in groundwater, Pe is effective precipitation, which is the total precipitation
293 minus runoff amount of the period

294 In this study, the recharge calculation using the CMB has been made by subdividing the
295 basin into southern, eastern, northern, and western catchments. Hence, the average chloride
296 concentration in the analyzed groundwater and rainfall sampled in the specific sub-area is
297 considered. These subdivisions are based on similar runoff characteristics and runoff coefficients
298 in the distinguished catchments (Dessie et al., 2015). The mean annual rainfall within the
299 respective areas, and mean annual runoff estimated by Dessie et al. (2015) separately for the four
300 sub-areas are considered for the effective precipitation calculation.

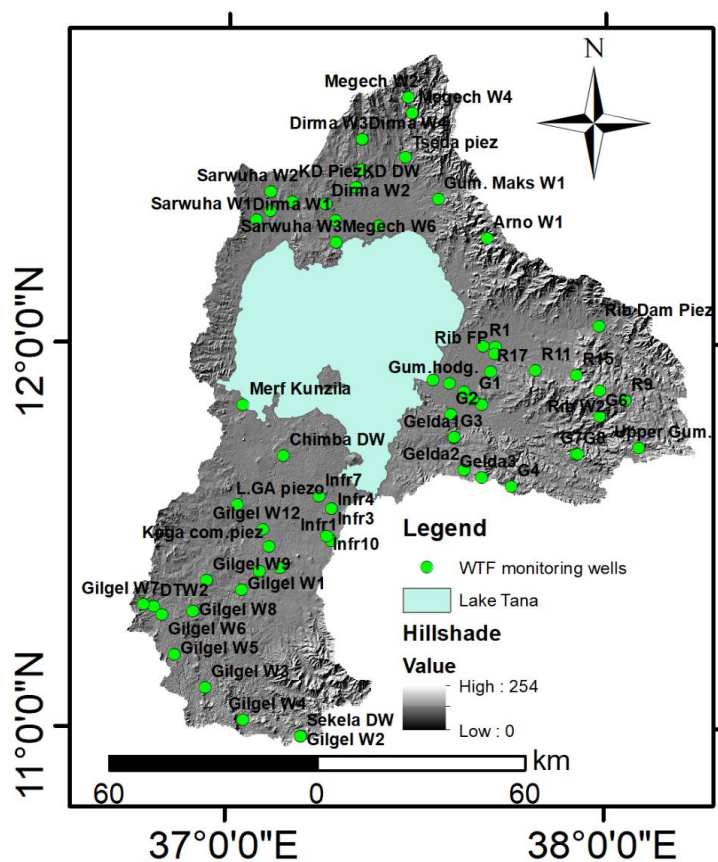
301 3.2.1. Data for WTF and CMB methods

302 In this study, the water table fluctuation and the chloride mass balance methods are also used
303 to estimate recharge besides the WetSpas water balance model, to independently verify and
304 compare the spatial estimation. Hence, high-frequency water level data logging and water
305 sampling for chloride and associated chemicals have been executed.

306 Water level data were being collected from May 2017 to June 2019 using 65 shallow hand-
307 dug and piezometer wells using community-based manual daily measurement and automatic
308 measuring sensors at every half an hour interval. We trained the local people, mostly the well
309 owners, and sometimes their neighbors in cases where the owners are illiterate. Afterward, we
310 supplied them with a measuring meter and a rope tied with a steel rod having a length of about
311 half a meter. Every morning before fetching water, they insert this rope tied with the steel rod into
312 the well until it reaches some depth below the water level, and then immediately get it out and
313 measure the depth from the head of the well to the tip of the moist surface on the metal plate. 52
314 of the monitoring wells were large diameter hand-dug wells and had been measured manually



315 using such simple equipment, whereas the other 13 wells were being monitored using automatic
316 data loggers. These 13 wells were both shallow piezometers and deep wells (9 shallow piezometers
317 and 4 shallow borehole wells). The measuring time interval for the manual readings was daily, and
318 for the automatic logging, it was every half an hour. Some of the hand-dug wells are active water
319 supplying wells where the owners fetch water for domestic and/or backyard irrigation purposes.
320 Hence, we order our data recorders to measure the static water level in the early morning when it
321 is preceded by long non-fetching hours (when full recovery is maintained). These monitoring wells
322 are well distributed over the studied basin and representing the various geological and
323 topographical settings.



324

325 *Fig. 6. location of 65 monitoring wells used for WTF estimation. Monitored both manually and*
326 *automatically by data logger sensor. Fairly distributed depending on topography and geology.*



327 Water sampling for chemical analysis of the groundwater had been undertaken from 2016 to
328 2019. The sampling sites were distributed throughout the study area representing the different
329 aquifer settings, considering geology and topography. Similarly, rainfall samples had been
330 collected in similar periods at the lower, middle, and upper topography of the basin so that possible
331 topographical influences on the rainfall water chemistry are taken into consideration. In total, about
332 255 groundwater samples and 25 rainfall samples have been collected and analyzed at Ghent
333 University, Department of Geology, Laboratory of Applied Geology and Hydrogeology. Good
334 handling practices of the samples during sampling, storage, and analysis were considered so that
335 evaporation which would increase the concentration of chloride through artificial means is absent.

336 4. Result and discussion

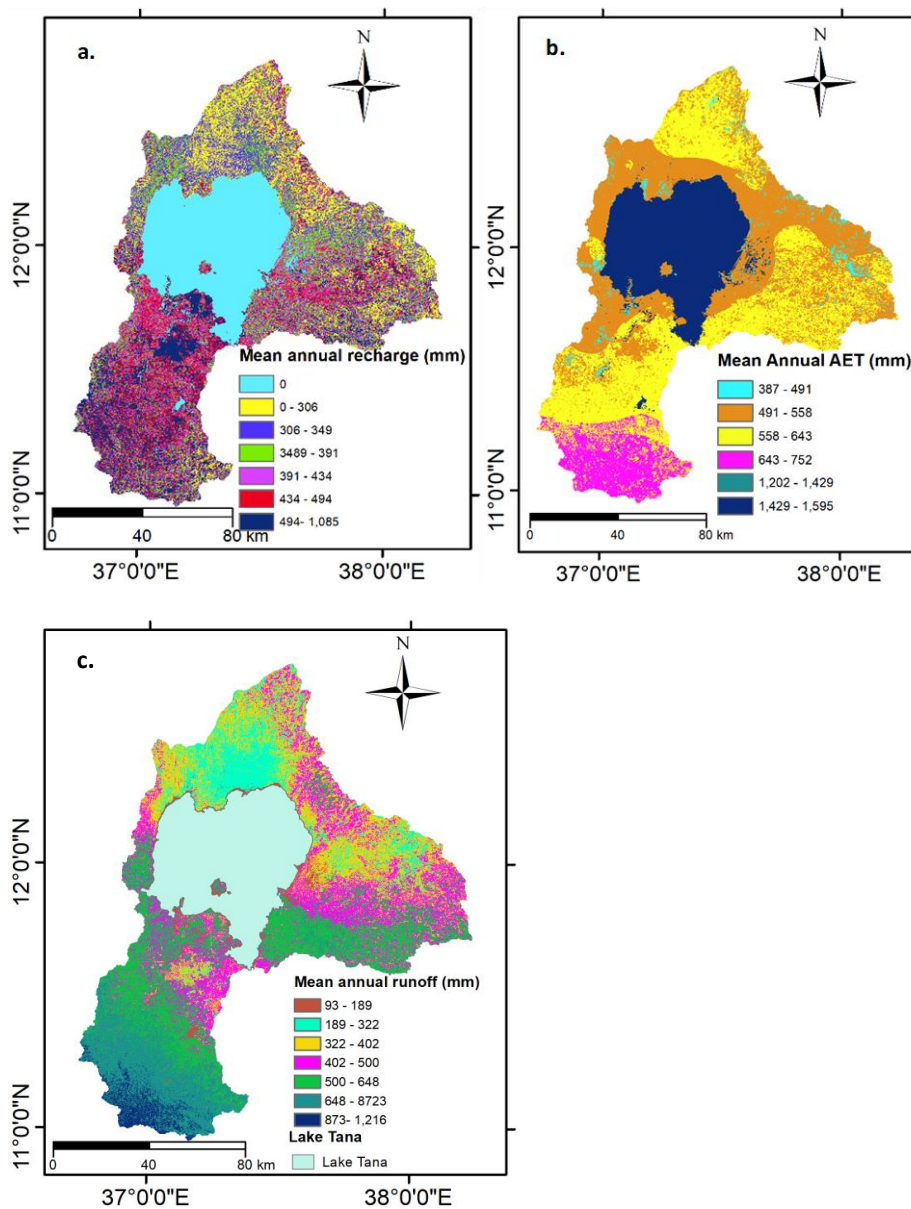
337 4.2. Spatial and temporal variation of groundwater recharge and other water 338 balance components

339 The calibrated WetSpa model developed using the present land use (2014 land use) presents
340 different water balance components. Among them, the annual groundwater recharge, runoff, and
341 evapotranspiration as spatially distributed digital maps are the primary ones. The annual
342 groundwater recharge ranges from 0 mm to 1085 mm (Fig. 7a) and has a mean value of 315 mm
343 (22% of rainfall amount). Recharge is assumed 0 mm at water bodies and wetlands in the WetSpa
344 model. Hence, recharge is 0 mm at Lake Tana and a dam reservoir in the Gilgel Abay catchment
345 and wetlands in the lower reaches of Rib river catchment (Fig. 4c). No recharge at water body is
346 the general assumption of the WetSpa model. Fortunately, this assumption is in line with
347 previous studies (e.g. Kebede et al., 2006; Mamo, 2015; SMEC, 2008), which had concluded
348 that there is insignificant percolation beneath the lake floor. Higher recharge is estimated on the
349 southern (Gilgel Abay) and eastern (Gumara) river catchments (Figs. 1b and 7a), and lower on the
350 northern part of the Lake Tana basin. This is mainly due to the lower rainfall amount in the northern
351 catchments compared to southern catchments (Figs. 3b and 7a). Next to the rainfall, the spatial
352 distribution of the recharge seems highly controlled by the slope angle, followed by the soil type,
353 and the land use type. Forest land covering only 1.8% has high recharge (mean annual of 542 mm).
354 Cultivated land and water body consisting of about 49% and 21% of the total areal coverage, have
355 annual mean recharge values of 370 mm and 0 mm, respectively, dominating over the total average
356 value. Clay soil type, covering about 77% of the total basin area, has a mean annual value of about



357 276 mm, the lowest amount estimated compared to all other soil types. The major recharge is
358 taking place during the summer season while only a small amount recharges during the winter
359 about 237 mm is recharged in the summer and 78 mm in the winter seasons. The mean annual
360 recharge is about 22% of the total mean basin precipitation.

361 The mean annual runoff for the whole basin is about 416 mm, accounting for about 29% of the
362 average precipitation. About 92% of the runoff is taking place during the summer season, while
363 the remaining is taking place during the long winter season. Relatively higher runoff is observed
364 in the southern and eastern basins, and lower runoff has been noted in the northern and northeastern
365 (Rib) river catchments (Fig. 7c). This is in line with the study by Dessie et al. (2015). In some
366 areas (e.g. in northern and northeastern), low runoff value has been observed on the cultivated land
367 and clay soil types where a high runoff coefficient is expected (Figs. 4c, 5a, and 7c). This is due
368 to the relatively low rainfall amount on these parts of the Lake Tana basin (Fig. 3b). This shows
369 that compared to the rainfall, the soil type and the land use have less influence over the runoff. The
370 rainfall amount is highly controlling the spatial distribution of runoff (Figs. 3b and 7c). The zonal
371 statistics for the land use and soil classes types show a high variation of runoff over the single class
372 types. For example, for clay soil with cultivated land cover type, the runoff ranges from 212 mm
373 to 1216 mm (15%-84% of mean rainfall), and with an average of 485 mm accounting for about
374 34% of the rainfall. This variation is found mainly due to the variation in the rainfall amount,
375 which is varying from 1097 mm to 2155 mm for the aftermentioned soil and land use class
376 combination. However, it does not mean that the other runoff controlling variables such as the
377 slope are not playing a significant role for such variations.



378
379 *Fig. 7. Long-term mean annual groundwater recharge(a), mean annual actual evapotranspiration (b),*
380 *and mean annual runoff (c) spatial maps produced from the WetSpass water balance model.*

381 The evapotranspiration of the Lake Tana basin is mainly the sum of the lake and wetland
382 direct evaporation and evapotranspiration over the other land cover types. The mean evaporation
383 over the lake is about 1485 mm. In the WetSpass model, the Penman method is used to estimate



384 the open water evaporation (Batelaan et al., 2007). The average total evapotranspiration over the
 385 basin is 770 mm, which is 53% of the mean basin precipitation. About 56% of total
 386 evapotranspiration is happening during summer and the other 44% occurs during winter. The mean
 387 evapotranspiration of the basin is about 52% of the mean potential evapotranspiration. The spatial
 388 distribution of the evapotranspiration over the basin is highly controlled by the rainfall and the
 389 land cover types relative to the other physical and meteorological variables (Figs. 3b, 4c, and 7b).
 390 It is higher over the lake and wetlands because it is open water where there is no limitation of water
 391 availability, and evaporation is equal to the potential evaporation capability of the air. The variation
 392 over the lake (Fig. 7b) is due to the variation of the potential evaporation (Figs. 3b and c). Next to
 393 the water bodies and wetlands, grassland, forest, bush and shrubland cover types have high
 394 evapotranspiration values.

395 The direct lake water evaporation is compared with other studies estimated by different
 396 methods (Table 2). The result is very close to that of Kebede et al. (2006) and Chebud and Melesse
 397 (2009) which both used the similar Penman method, and similar time scale (Table 2). However, it
 398 is lower than the value estimated by Dessie et al. (2015) which used recent data from six stations.
 399 This could be due to the application of different period data (from 2012-2013 while it is from
 400 2005-2018 in this study) or the time scale applied (seasonal versus daily) for the calculation or it
 401 might be due to the method they used (Table 2). Time scale affects evapotranspiration calculations,
 402 which are higher for fine time scales (e.g. daily), and relatively lower for coarser time scales (e.g.
 403 seasonal or monthly) (Bakundukize et al., 2011; Yenehun et al., 2020).

404 *Table 2. Simulated mean annual evaporation over the lake of the WetSpass water balance model, and other studies.*
 405 *The time scale for the modeling, the period that the meteorological data used and the number of meteorological*
 406 *stations, and the estimation technique are indicated.*

Literature	Timescale	Data period used	Number of stations	Estimation method applied	Annual over-lake evaporation (mm)
This study	seasonal	2005-2018	7	Penman (WetSpass)	1458
Wale et al. (2009)	daily	1992-2003	2	Penman-combination equation	1690



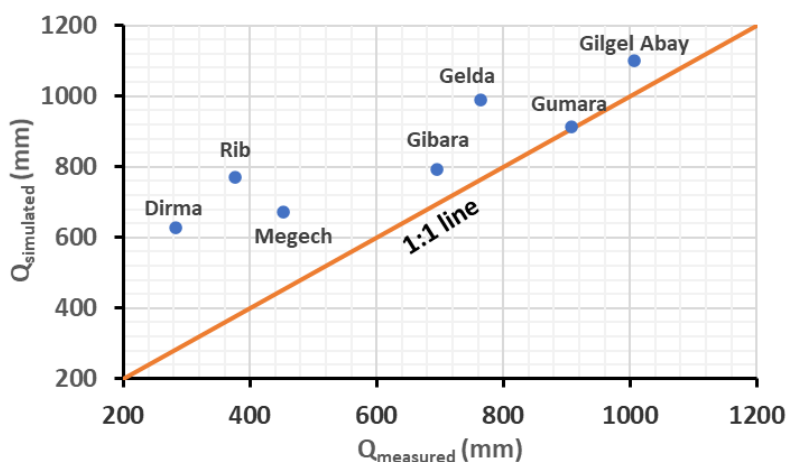
Rientjes et al. (2011)	daily	1994–2003	1	Penman-combination equation	1563
Kebede et al. (2006)	daily	1960–1992	1	Penman	1478
SMEC (2008)	monthly	1960–2005	2	Penman	1697
	monthly	1960–1995		Energy balance	1657
Mamo (2015)	monthly	1995–2009	1	Penman	1544
Setegn et al. (2008)	daily	1978–2004	not explicitly mentioned (probably 2)	Hargreaves	1248
Dessie et al. (2015)	daily	2012–2013	6	Penman-combination	1789
Chebud and Melesse (2009)	monthly	not mentioned	1	Penman	1458

407 **4.2.1. Model verification**

408 The developed model is verified using two ways. First, the annual total river discharge
 409 observed by Dessie et al. (2015), using the daily time scale data of river discharge of 2012-2013
 410 at seven major rivers, is compared with the corresponding WetSpass model results. These data
 411 have been used for the calibration of the model. The river discharge measured by Dessie et al.
 412 (2015) for these major perennial rivers is the total flow amount (comprising both surface and
 413 baseflow). However, the WetSpass model calculates the runoff (only the surface runoff) but not
 414 the total discharge. Hence, to estimate the total river flow at the catchment outlets of each river,
 415 we applied a similar technique that Gebreyohannes et al. (2013) had followed. Based on
 416 groundwater balance in the aquifers, the long-term average annual groundwater drainage and
 417 possible abstractions are equal to the long-term average annual recharge. Given the river gauging
 418 stations are usually at the groundwater discharge zones (on the floodplain), the flow measurements
 419 are assumed to catch the baseflow component except for a very small amount that may pass
 420 through deep percolations. Besides, the groundwater abstractions using different shallow and deep
 421 wells can be assumed small compared to natural drainage and recharge as there is no large
 422 development of the groundwater in the basin. Using ArcGIS 10.3 tools, both annual runoff and
 423 groundwater recharge outputs of the WetSpass model, are accumulated at the river outlets. Finally,
 424 the accumulated raster maps of runoff and recharge for each major catchment are summed up to
 425 produce the spatial total river discharge map. The total river discharges estimated in this study and
 426 those observed by Dessie et al. (2015) are compared (Fig. 8). The overall coefficient of
 427 determination (R^2) between the simulated and the observed river discharge values of the different



428 rivers is about 80% however, for Rib, Dirma, Gelda and Megech river catchments, the simulation
429 by WetSpass is higher compared to the observation by Dessie et al. (2015) (Fig. 8). This could be
430 due to significant deep percolation of the groundwater that is not caught by the river flow
431 measurements i.e. the baseflow is far less than the groundwater recharge.. The model is best
432 simulated for Gilgel Abay and Gumara rivers (Fig. 8). This could be due to the catching up of the
433 baseflow in the flow measurements as most of the groundwater discharges through different
434 springs in the lower reach of the rivers. Similarly, SMEC (2008), and later Dessie et al. (2015,
435 2014) came up with the conclusion that there is significant groundwater contribution for Gilgel
436 Abay and Gumara rivers flow while only little for Megech and Rib. Furthermore, Setegn et al.
437 (2008) had estimated the groundwater (as baseflow) contribution of the whole basin to be 50% of
438 the total river inflow to the lake. It should be noted that the WetSpass model applied is quasi-
439 steady state, and uses long-term average seasonal rainfall, whereas, in reality, the rainfall
440 characteristics (intensity, frequency and duration) vary within fine time scales. This is limiting the
441 effectiveness of the model in simulating runoff.

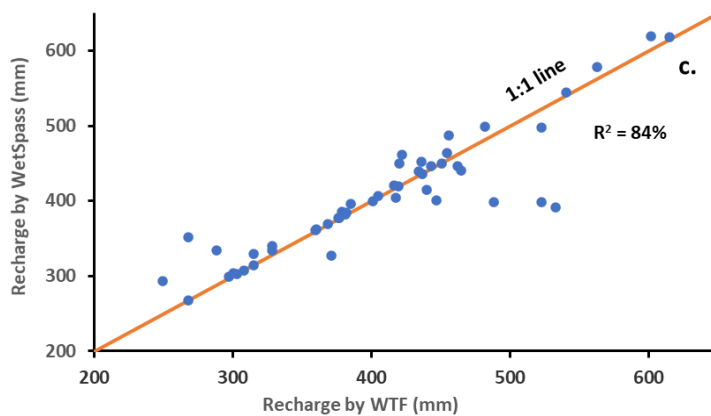
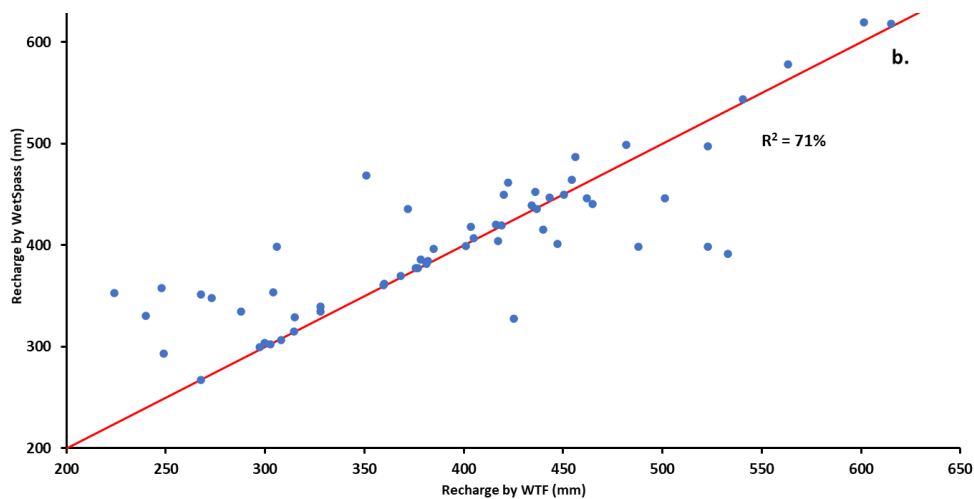
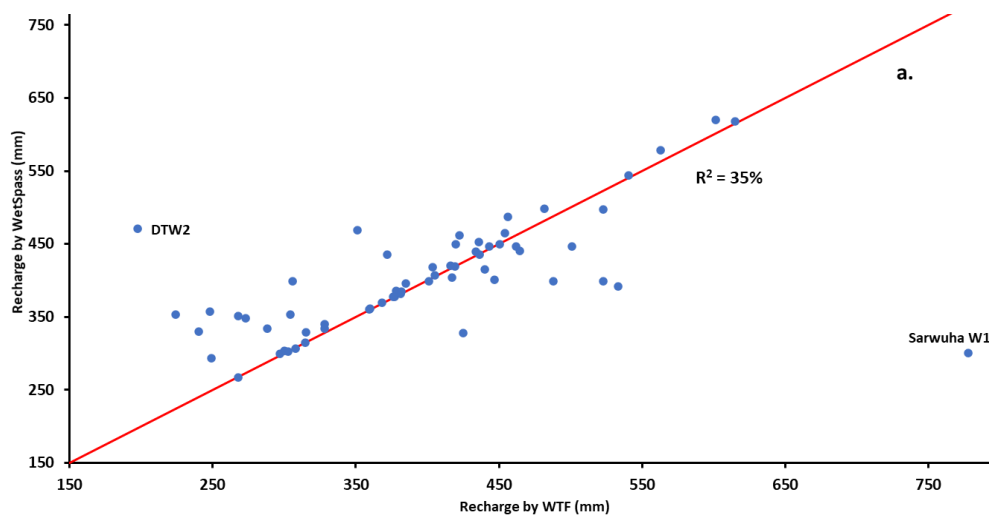


442

443 Fig. 8. A 1:1 line between measured mean annual river flow obtained from Dessie et al. (2015) and
444 simulated mean annual river flow by WetSpass water balance model for the major rivers in the Lake Tana
445 basin. The simulated river flow is calculated by summing up the runoff and the groundwater recharge
446 values of each catchment by assuming all the recharge in the upper catchments emerges as an outflow in
447 the lower floodplain parts.



448 The second way that the developed WetSpass model verification made is through its
449 performance in estimating groundwater recharge. The point recharge estimated using the WTF
450 method has been used to compare the model performance at those points. The extracted recharge
451 values of the model were correlated against the WTF results calculated at 65 monitoring stations
452 (Fig. 9a). The overall correlation was fair (with a coefficient of determination, $R^2 = 35\%$).
453 However, Yenehun et al. (2020) evaluated the performance of the WetSpass model in estimating
454 recharge at a small catchment in the upper Gilgel Abay river catchment and found that the
455 technique is less effective at storage controlled flat floodplain areas and at aquifers where focused
456 recharge (through rock fractures) is an important recharging mechanism. Therefore, we excluded
457 WTF results estimated at aquifers on those topographies, and then the correlation coefficient (R^2)
458 is found to be 84% (Fig. 9c). When only two wells located at storage controlled floodplain aquifer
459 named DTW2 and at exceptionally highly fractured aquifer called Sarwuha W1 (Fig. 6) are
460 excluded, the R^2 raised to 71% (Fig. 9b). Hence, the WetSpass method is found effective in
461 estimating the groundwater recharge in most parts of the study basin. However, at the flat
462 floodplain alluvial aquifer and fractured rock aquifers where the hard rock is exposed to the
463 surface, water balance techniques such as the WetSpass are found less effective.





465 *Fig. 9. a) A plot of mean annual recharge by WTF and WetSpass methods at all groundwater monitoring wells.*
466 *The recharge values estimated using WetSpass are extracted at 65 water level monitoring points. It has a*
467 *total correlation of 35%. b) A plot of mean annual recharge by WTF versus extracted recharge by*
468 *WetSpass method for monitoring points excluding Sarwuha W1 and DTW2 those strongly affected by*
469 *focused recharge and limited with aquifer storage, respectively. c) A plot of mean annual recharge by*
470 *WTF versus extracted recharge by WetSpass method for monitoring points excluding those affected by*
471 *focused recharge and those which are storage controlled on the flat floodplain areas. It has a correlation*
472 *coefficient of 84%.*

473 **4.3. Effect of land use change on groundwater recharge and other water** 474 **balance components**

475 The effect of land use change on groundwater recharge, runoff, and evapotranspiration has
476 been assessed in this study. This assessment has been made using similar long-term average
477 meteorological data, and hence possible variation due to temporal increasing or decreasing of the
478 meteorological variables have not been taken into consideration.

479 The value of water balance terms changes with land use changes. There is a decrease in
480 recharge by 13 mm or $195.9 \times 10^6 \text{ m}^3$ in the years 1986-2014 (Table 3) in the Lake Tana basin. This
481 is about 4% of the mean annual recharge estimated with the applied WetSpass model. This is inline
482 with the increase of cultivated land area (from 36.7% to 49%), mainly from grass, bush and shrub,
483 and forest lands. Similarly, there is an increase of runoff but it is only by 4 mm or $60.3 \times 10^6 \text{ m}^3$ in
484 the 28 years (about 1% of the total mean runoff). Similarly, the evapotranspiration shows an
485 increment by 9 mm or $135.6 \times 10^6 \text{ m}^3$ in these 28 years (about 1.2% of the total mean annual AET).
486 The trend is in line with the studies by Abate et al. (2017), Enku et al. (2014), Gebremicael et al.
487 (2013), Hurni et al. (2005), Tesemma et al. (2010), and Woldesenbet et al. (2017), which showed
488 the shifting of the river discharge more to overland flow mechanism in the last four to five decades
489 in the upper Blue Nile basin. However, the rate of hydrological change found in this study is
490 relatively small compared to the rate of land use change. This reinforces the idea that the land use
491 is not the primary important controlling factor compared to rainfall amount (discussed above in
492 detail). Similarly, Birhanu et al. (2019) found a negligible change of the water balance components
493 for Gumara catchment for the land use change of 1986-2015 using HBV model. Gashaw et al.
494 (2018) had also evaluated the effect of changing land use on the hydrology of Andassa catchment
495 (neighboring small catchment, south of Lake Tana basin) over the same period (1986-2015) using




496 SWAT model. Compared to this study, they found a similar amount of reduction in baseflow
497 (supposed to be equivalent to groundwater recharge), but a bit more runoff increment.

498 *Table 3. Long-term mean seasonal and annual groundwater recharge, runoff, and evapotranspiration values*
499 *simulated for land use of the years 1986, 2000, and 2014 using the WetSpa water balance model.*

Year	season	recharge (mm)	runoff (mm)	total evapotranspiration (mm)
1986	summer	247	379	424
	winter	81	33	337
	annual	328	412	761
2000	summer	243	381	427
	winter	79	33	338
	annual	322	414	765
2014	Summer	237	383	428
	winter	78	33	342
	annual	315	416	770

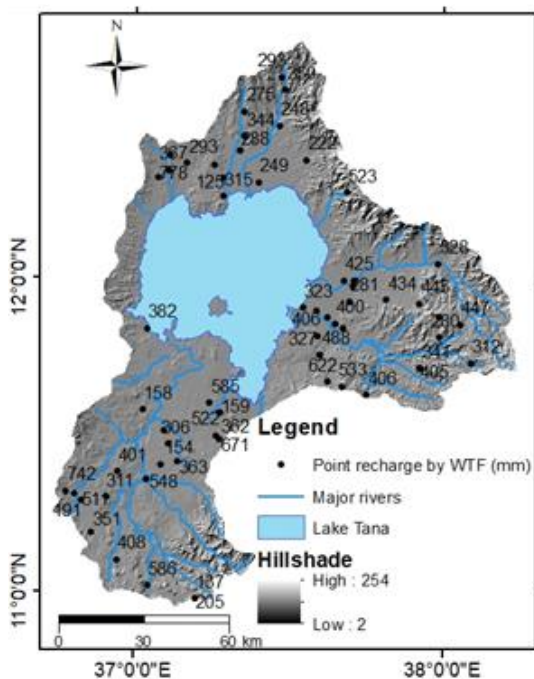
500 **4.4. Groundwater recharge estimation using F and CMB methods**

501 The aquifer type, location, and hydrograph response for recharging periods for the 65 wells
502 are checked, and found as they are more or less fulfill the assumptions of the WTF method for
503 recharge estimation discussed in detail by Healy and Cook (2002). The seasonal recharge values
504 calculated for 2017, 2018, and some for 2019, are averaged out. Many rises and declines within
505 the overall recharging season are not considered. Only the seasonal highest rise and extrapolated
506 antecedent decline during the highest rise (using the graphical technique) has taken into account.
507 As a result, the calculated recharge is the total recharge that joined the groundwater.

508 The specific yield was estimated both using a literature compilation of Johnson (1967), and
509 through an empirical formula developed by Beretta and Stevenazzi (2018) for the wells where
510 pumping tests had been executed. The resulting specific yield values are highly variable depending
511 on primarily geology and degree of weather  Hydrogeologically, the shallow monitoring wells
512 are placed on four hydrogeological units: weathered basaltic regolith, pyroclastic rocks, fractured
513 Quaternary basalt (with intermediate weathering grade), and alluvio-lacustrine formations. The
514 Quaternary basalt was found with the highest Sy value (ranging from 0.08 to 0.1), while for the



515 pyroclastic and alluvio-lacustrine deposits, values as low as 0.02 and as high as 0.074 were found.
516 The weathered basaltic regolith has a specific yield ranging from 0.04 to 0.08.



517

518 *Fig. 10. Point values of annual groundwater recharge estimated at 65 groundwater level monitoring wells.*
519 *The wells include shallow hand-dug wells, piezometers, and a few boreholes being monitored both*
520 *manually and using automatic pressure transducer device.*

521 The mean annual groundwater recharge using the WTF ranges from 125 mm to 778 mm,
522 accounting for about 9% to 54% of the mean basin rainfall. In general, the southern and eastern
523 (Gumara river catchment) part of the Lake Tana basin has higher recharge than the northern part
524 (Fig. 10). This is also similar to the result of the WetSpass model (Fig. 7a). It has an overall basin
525 average of 369 mm (26% of the rainfall), which is a bit higher than the mean average estimated by
526 the WetSpass model (22%). This could be due to the ability of the WTF method to catch up the
527 focused recharge through rock fractures, and/or lateral groundwater flow besides the diffuse
528 recharge from the direct precipitation that Yenehun et al. (2020) had thoroughly discussed. The
529 spatial variation of recharge depends on topography and geology. In steep sloping topography
530 aquifers, where low recharge is expected, higher recharge values by WTF compared to WetSpass
531 is estimated (Figs. 5c and 10). This is due to the additional recharge from the upstream area by



532 lateral groundwater flow in addition to the diffuse recharge from the direct rainfall, therefore,
533 on the flat floodplain areas, the recharge estimated by the WTF is small. This is due to the
534 limitation of the aquifer storage. It means the aquifer is more or less fully recharged in the early to
535 middle of the recharge period (usually end of July to mid-August) but the model keeps on adding
536 the recharge as there is unlimited aquifer storage. In general, the WetSpass method is less effective
537 in the fractured aquifers where focused recharge is the important recharging mechanism and on
538 flat floodplain areas, which disregards both the storage limitation in the flat floodplain alluvial and
539 additional focused recharge in the fractured rock aquifers. In addition, it performs less in steeply
540 sloping aquifers where fast groundwater flow accumulates additional recharge through lateral
541 groundwater flow.

542 Similar to WetSpass and WTF methods, the recharge calculation using the CMB method
543 shows strong spatial variability. The groundwater recharge in the southern and eastern catchments
544 is higher than in the northern, and western catchments (Table 4). The mean annual recharge by the
545 CMB method is about 346 mm (24% of the rainfall). The spatial distribution is more or less similar
546 to the spatial distribution map simulated by WetSpass (Fig. 7a), and the point recharge distribution
547 of the WTF method (Fig. 10).

548 *Table 4. Estimated mean annual groundwater recharge amount using the CMB method for the different catchments*
549 *grouped based on similar rainfall characteristics.*

Catchments	Number of analyzed GW points	Groundwater recharge (mm)
Southern	51	404
Eastern	65	355
Northern	15	164
Western	7	206

550 **4.5. Summarizing groundwater recharge estimations by the different** 551 **methods and comparing with other similar studies**

552 The mean annual groundwater recharge values found with the three methods are 311 mm for
553 WetSpass, 369 mm for WTF, and 345 mm for CMB. The WetSpass value ranges from 0 mm to
554 1085 mm, WTF ranges from 125 mm to 778 mm, and CMB from 164 mm to 404 mm. The
555 relatively smaller range for CMB is due to the consideration of average values in the four



556 distinguished zones rather than at 138 groundwater sampling points. Otherwise, the range of values
557 would have been higher, given the wider range of chloride values (0.3 to 12.5 mg/l) of the
558 groundwater samples. The heterogeneity in recharge processes and recharge rates over the basin
559 is well notified by the higher range of values by the WetSpass and WTF methods.

560 Generally, recharge in the eastern and southern catchments is higher than in the northern
561 catchments (Table 5), primarily due to higher rainfall and favorable geology (highly fractured
562 Quaternary basalt) (Fig. 2). The recharge by CMB in the northern, and somewhat in the western
563 part is much smaller compared to the values by the other two methods (Table 5). This could be
564 due to some recharge from the river water which elevates the chloride concentration of the
565 groundwater which hence decreases the recharge value according to Eq. 5. The chloride
566 concentration in the river water is higher due to exposure to open water evaporation before
567 infiltration and percolation to the groundwater zone.

568 *Table 5. mean annual groundwater recharge values estimated for the different catchments by all CMB, WetSpass*
569 *and WTF methods.*

Catchments	Groundwater recharge by CMB (mm)	Groundwater recharge by WetSpass (mm)	Groundwater recharge by WTF (mm)
Southern	404	453	439
Eastern	355	372	435
Northern	164	315	303
Western	206	357	445

570 There are other recharge studies performed on different sub-catchments of the Lake Tana
571 basin. Abiy et al. (2016) applied a SWAT model for Rib and Gumara catchments and estimated
572 recharge to be 451 mm and 414 m, respectively (Table 5). In the WetSpass model of this study,
573 352 mm for Rib, and 392 mm for Gumara are estimated, a bit smaller than the study by Abiy et al.
574 (2016). Yenehun et al. (2020) applied four different techniques to estimate recharge on the upper
575 part of Gilgel Abay catchment, and hence, 431 mm, 477 mm, and 462 mm, were estimated as mean
576 annual values using SM (soil moisture balance), CMB, and WetSpass. In the WetSpass model of
577 this study, 453 mm is the recharge amount for the whole Gilgel Abay catchment (Table 5), which
578 is very close to the result by Yenehun et al. (2020). Similarly, Yenehun et al. (2020) applied the
579 WTF method and estimated annual value ranging from 157 mm to 760 mm. Walker et al. (2019)



580 calculated the natural groundwater recharge using nine different methods in the Dangila area
581 (upper part of Gilgel Abay catchment). They estimated the mean annual recharge amount in the
582 range of 280–430 mm. Nigate et al. (2020) applied the WTF, CMB and SMB methods on Infranz
583 catchment, which is a small river catchment in the southern part of Lake Tana basin (Fig. 1). They
584 estimated 436 mm by CMB, values ranging from 400 and 800 mm by WTF, and 748 mm by SMB
585 as annual mean values. The results by these studies are more or less similar to the values found in
586 this study for those specific study areas. In the Infranz catchment, groundwater recharge is higher
587 than average, due to the focused recharge by fractured Quaternary basalt besides the direct
588 recharge. On the other hand, Mamo (2015) applied the CMB method for the whole Tana basin,
589 and estimated recharge to be 284 mm, which is underestimated compared to our results. This could
590 be due to using deep well groundwater chloride data which are more mineralized or due to rainfall
591 sampling period i.e. chloride concentration of rainfall is highly variable depending season

592 Different authors presented recharge values for different parts of Ethiopian aquifers. Ferede
593 et al. (2020) have applied WTF and CMB techniques at a small catchment on a rift valley volcanic
594 aquifer. They estimated recharge at 35% and 20% of rainfall, respectively by WTF and CMB,
595 while it is 26% for the former and 24% for the latter in our study. These results are comparable.
596 The relatively higher recharge by WTF in this rift valley volcanic aquifer could be due to the more
597 open fractures in Quaternary basalt that have significant focused recharge. The geology of rift
598 valley is Quaternary volcanic rocks where open fissures and fractures are very common (Paola,
599 1972). Tilahun et al. (2009) applied the WetSpss model on an area predominantly containing
600 sedimentary and basement rock aquifers in eastern Ethiopia. They estimated the mean annual
601 recharge value at 5% of rainfall. Similarly, Gebreyohannes et al. (2013) applied the same method
602 on sedimentary rock aquifers in northern Ethiopia, and found 6% of rainfall amount. Both
603 estimates are too small compared to this study. This could be due to the high-intensity nature of
604 the rainfall (especially for the former) as well as the focused recharge through faults, bedding
605 surfaces, and joints, which is characteristic of the geology of these areas and which water balance
606 models like WetSpss fail to capture. Demlie et al. (2007a) applied the CMB method, and found
607 23% of rainfall as a recharge value in a similar volcanic aquifer in central Ethiopia, which is close
608 to our result (24% of rainfall). Using unsaturated zone chloride measurement, supported by stable
609 isotopes, they quantified a significant amount of focused recharge at areas where faults and joints



610 dominate. These all assert our finding that water balance methods are less effective in estimating
611 recharge over areas where recharge by preferential flow is common.

612 **5. Conclusion**

613 The physically-based water balance model, WetSpass has effectively been applied to simulate
614 the water balance components of Lake Tana basin, containing the largest lake of Ethiopia. The
615 model simulates the mean annual major river inflows with a coefficient of determination (R^2) of
616 80%. The model better simulated flows for the Gumara and Gilgel Abay river catchments than for
617 the other catchments where deep percolation might conceal the base flow from measurement by
618 the gauging stations. On the other hand, the WetSpass model applied is a quasi-steady state that
619 used long-term average seasonal rainfall amounts, though the rainfall characteristics vary within
620 fine time scales. This might limit the effectiveness of the model in simulating runoff amounts. The
621 annual groundwater recharge using WetSpass ranges from 0% of rainfall, at the water bodies where
622 infiltration is impossible, to 57% in the flat, silty loam, and bushland cover type. It has a mean
623 annual value of 315 mm (22% of the precipitation amount), of which 237 mm is recharged in
624 summer and the other 78 mm in the winter season. Similarly, the WTF and CMB methods have
625 also shown strong spatial variability, with higher recharge values in the southern and eastern
626 catchments, and lower in the northern and partly in the western parts, primarily due to rainfall
627 distribution and geology. There is good correlation between point recharge values by the WTF
628 and extracted recharge from the WetSpass spatial maps. However, there is a high disparity on
629 wells located on the storage-controlled flat floodplains and focused recharge affected fractured
630 rock aquifers. Hence, though water balance models estimate recharge at fine spatial scales that
631 help for water management in specific areas, its capacity is limited for aquifers where only diffuse
632 recharge is the main recharging mechanism and for those aquifers that are not fully saturated early
633 in the recharge period.

634 The mean annual runoff for the whole basin is about 416 mm (29% of the average
635 precipitation) and evapotranspiration is about 770 mm, which is 53% of the mean basin
636 precipitation. The precipitation amount is highly controlling the spatial distribution of the runoff,
637 more than the land use and soil. The mean evaporation over the lake is about 1485 mm. The spatial
638 distribution of the evapotranspiration over the basin is highly controlled by the rainfall and the



639 land cover types. The hydrology of the basin has not much changed in the last three decades though
640 cultivated land has expanded significantly.

641 **Author Contribution**

642 **Alemu Yenehun:** conceptualization, investigation, formal analysis, and writing - original draft

643 **Mekete Desssie:** project administration, conceptualization and investigation, writing- review and
644 editing

645 **Fenta Nigatie:** conceptualization and investigation, writing- review and editing

646 **Ashebir Sewale Belay:** conceptualization and investigation

647 **Mulugeta Azeze:** conceptualization, writing- review and editing

648 **Marc Van Camp:** conceptualization, formal analysis and Software

649 **Derbew Fenetie Taye:** data collection

650 **Desale Kidane:** writing- review and editing

651 **Enyew Adgo:** project administration, funding acquisition, writing- review and editing

652 **Jan Nyssen:** project administration, funding acquisition, writing- review and editing

653 **Ann van Griensven:** conceptualization, investigation

654 **Kristine Walraevens:** conceptualization, writing- review and editing, project administration and
655 supervision, validation.

656 **Competing interests**

657 The authors declare that they have no known competing financial interests or personal
658 relationships that could have appeared to influence the work reported in this paper.

659 **Acknowledgment**

660 This research work is funded by the Belgian Development Cooperation (VLIR-UOS)
661 through the BDU-IUC project. Hence, we would like to thank you VLIR-UOS for the funding,
662 and the project staff for facilitating our fieldwork activities. Furthermore, we want to extend our



663 thanks to our monitoring well data recorders, who had been consistently recording the data. We
664 would like also to extend our thanks to the Ethiopian Meteorological Agency, Bahir Dar Branch,
665 and different zonal and woreda water offices that help during monitoring well installation and data
666 recording personnel recruitment.

667 **References**

- 668 Abate, M., Nyssen, J., Moges, M.M., Enku, T., Zimale, F.A., Tilahun, S.A., Steenhuis, T.S., 2017. Long-
669 Term Landscape Changes in the Lake Tana Basin as Evidenced by Delta Development and
670 Floodplain Aggradation in Ethiopia. *L. Degrad. Dev.* 28, 1820–1830.
- 671 Abiy, A.Z., Demissie, S.S., Charlotte, M., Dessu, S.B., Melesse, A.M., 2016. Groundwater Recharge and
672 Contribution to the Tana Sub-basin, Upper Blue Nile Basin, Ethiopia, in: *Landscape Dynamics,*
673 *Soils and Hydrological Processes in Varied Climates.* pp. 463–481. [https://doi.org/10.1007/978-3-](https://doi.org/10.1007/978-3-319-18787-7)
674 [319-18787-7](https://doi.org/10.1007/978-3-319-18787-7)
- 675 ADSWE, 2015a. Tana sub basin integrated Land Use Planning and Environmental impact Study,
676 Technical Report: Land Use Land Cover and Change Detection.
- 677 ADSWE, 2015b. Tana sub basin Land Use Planning and Environmental Study Project, Technical Report
678 I: Soil Survey.
- 679 Alemayehu, T., Kebede, S., 2011. The role of geodiversity on the groundwater resource potential in the
680 upper Blue Nile River Basin, Ethiopia. *Environ. Earth Sci.* 64, 1283–1291.
681 <https://doi.org/10.1007/s12665-011-0946-7>
- 682 Allen, R.G., Pereira, L.S., Raes, D., Smith, M., 1998. Crop evapotranspiration-Guidelines for computing
683 crop water requirements-FAO Irrigation and drainage paper 56, FAO, Rome.
- 684 Allison, G.B., 1988. A Review of Some of the Physical, Chemical and Isotopic Techniques Available for
685 Estimating Groundwater Recharge, in: Springer. pp. 49–72.
- 686 Allison, M., Hughes, G., 1978. The use of environmental chloride and tritium to estimate total recharge
687 to an unconfined aquifer. *Aust. J. Soil Res.* 16, 181–195. <https://doi.org/10.1071/SR9780181>
- 688 Ashaolu, E.D., 2020. Spatial and temporal recharge estimation of the basement complex in Nigeria , West
689 Africa. *J. Hydrol. Reg. Stud.* 27, 100658. <https://doi.org/10.1016/j.ejrh.2019.100658>
- 690 Ayenew, T., Demlie, M., Wohnlich, S., 2008. Hydrogeological framework and occurrence of
691 groundwater in the Ethiopian aquifers. *J. African Earth Sci.* 52, 97–113.



- 692 <https://doi.org/10.1016/j.jafrearsci.2008.06.006>
- 693 Bakundukize, C., van Camp, M., Walraevens, K., 2011. Estimation of Groundwater Recharge in
694 Bugesera Region (Burundi) using Soil Moisture Budget Approach. *Geol. Belgica* 14, 85–102.
- 695 Batelaan, O., De Smedt, F., 2007. GIS-based recharge estimation by coupling surface-subsurface water
696 balances. *J. Hydrol.* 337, 337–355. <https://doi.org/10.1016/j.jhydrol.2007.02.001>
- 697 Batelaan, O., De Smedt, F., 2001. WetSpa: a flexible, GIS based, distributed recharge methodology for
698 regional groundwater modelling, in: *Impact of Human Activity on Groundwater Dynamics*. IAHS
699 Publ, pp. 11–18.
- 700 Beretta, G.P., Stevenazzi, S., 2018. Specific yield of aquifer evaluation by means of a new experimental
701 algorithm and its applications. *Ital. J. Groundw.* 24, 39–46. <https://doi.org/10.7343/as-2018-325>
- 702 Birhanu, A., Masih, I., van der Zaag, P., Nyssen, J., Cai, X., 2019. Impacts of land use and land cover
703 changes on hydrology of the Gumara catchment, Ethiopia. *Phys. Chem. Earth* 112, 165–174.
704 <https://doi.org/10.1016/j.pce.2019.01.006>
- 705 Chebud, Y.A., Melesse, A.M., 2009. Modelling lake stage and water balance of Lake Tana, Ethiopia.
706 *Hydrol. Process.* 23, 3534–3544. <https://doi.org/10.1002/hyp.7416>
- 707 Chorowicz, J., Collet, B., Bonavia, F.F., Mohr, P., Parrot, J.F., Korme, T., 1998. The Tana basin,
708 Ethiopia: Intra-plateau uplift, rifting and subsidence. *Tectonophysics* 295, 351–367.
709 [https://doi.org/10.1016/S0040-1951\(98\)00128-0](https://doi.org/10.1016/S0040-1951(98)00128-0)
- 710 Crosbie, R.S., Binning, P., Kalma, J.D., 2005. A time series approach to inferring groundwater recharge
711 using the water table fluctuation method. *Water Resour. Res.* 41, 1–9.
712 <https://doi.org/10.1029/2004WR003077>
- 713 Delin, G.N., Healy, R.W., Lorenz, D.L., Nimmo, J.R., 2007. Comparison of local- to regional-scale
714 estimates of ground-water recharge in Minnesota, USA. *J. Hydrol.* 334, 231–249.
715 <https://doi.org/10.1016/j.jhydrol.2006.10.010>
- 716 Demlie, M., Wohnlich, S., Ayenew, T., 2008. Major ion hydrochemistry and environmental isotope
717 signatures as a tool in assessing groundwater occurrence and its dynamics in a fractured volcanic
718 aquifer system located within a heavily urbanized catchment, central Ethiopia. *J. Hydrol.* 353, 175–
719 188. <https://doi.org/10.1016/j.jhydrol.2008.02.009>
- 720 Demlie, M., Wohnlich, S., Gizaw, B., Stichler, W., 2007a. Groundwater recharge in the Akaki catchment



- 721 , central Ethiopia : evidence from environmental isotopes ($\delta^{18}\text{O}$, $\delta^2\text{H}$ and $\delta^3\text{H}$) and chloride
722 mass balance. *Hydrol. Process.* 21, 807–818. <https://doi.org/10.1002/hyp.6273>
- 723 Demlie, M., Wohnlich, S., Wisotzky, F., Gizaw, B., 2007b. Groundwater recharge, flow and
724 hydrogeochemical evolution in a complex volcanic aquifer system, central Ethiopia. *Hydrogeol. J.*
725 15, 1169–1181. <https://doi.org/10.1007/s10040-007-0163-3>
- 726 Dessie, M., Verhoest, N.E.C., Pauwels, V.R.N., Adgo, E., Deckers, J., Poesen, J., Nyssen, J., 2015. Water
727 balance of a lake with floodplain buffering: Lake Tana, Blue Nile Basin, Ethiopia. *J. Hydrol.* 522,
728 174–186. <https://doi.org/10.1016/j.jhydrol.2014.12.049>
- 729 Dessie, M., Verhoest, N.E.C., Pauwels, V.R.N., Admasu, T., Poesen, J., Adgo, E., Deckers, J., Nyssen, J.,
730 2014. Analyzing runoff processes through conceptual hydrological modeling in the Upper Blue Nile
731 Basin , Ethiopia 5149–5167. <https://doi.org/10.5194/hess-18-5149-2014>
- 732 Dile, Y.T., Tekleab, S., Kaba, E.A., Gebrehiwot, S.G., Worqlul, A.W., Bayabil, H.K., Yimam, Y.T.,
733 Tilahun, S.A., Daggupati, P., Karlberg, L., Srinivasan, R., 2018. Advances in water resources
734 research in the Upper Blue Nile basin and the way forward: A review. *J. Hydrol.* 560, 407–423.
735 <https://doi.org/10.1016/j.jhydrol.2018.03.042>
- 736 Enku, T., Tadesse, A., Yilak, D.L., Gessesse, A.A., Addisie, M.B., Abate, M., Zimale, F.A., Moges,
737 M.A., Tilahun, S.A., Steenhuis, T.S., 2014. Biohydrology of low flows in the humid Ethiopian
738 highlands: The Gilgel Abay catchment. *Biol.* 69, 1502–1509. [https://doi.org/10.2478/s11756-014-](https://doi.org/10.2478/s11756-014-0462-9)
739 0462-9
- 740 Ferede, M., Haile, A.T., Walker, D., Gowing, J., 2020. Multi-method groundwater recharge estimation at
741 Eshito micro-watershed , Rift Valley Basin in Ethiopia. *Hydrol. Sci. J.* 65, 1596–1605.
742 <https://doi.org/10.1080/02626667.2020.1762887>
- 743 Gashaw, T., Tulu, T., Argaw, M., Worqlul, A.W., 2018. Modeling the hydrological impacts of land
744 use/land cover changes in the Andassa watershed, Blue Nile Basin, Ethiopia. *Sci. Total Environ.*
745 619–620, 1394–1408. <https://doi.org/10.1016/j.scitotenv.2017.11.191>
- 746 Gebremicael, T.G., Mohamed, Y.A., Betrie, G.D., van der Zaag, P., Teferi, E., 2013. Trend analysis of
747 runoff and sediment fluxes in the Upper Blue Nile basin: A combined analysis of statistical tests,
748 physically-based models and landuse maps. *J. Hydrol.* 482, 57–68.
749 <https://doi.org/10.1016/j.jhydrol.2012.12.023>
- 750 Gebreyohannes, T., De Smedt, F., Walraevens, K., Gebresilassie, S., Hussien, A., Hagos, M., Amare, K.,



- 751 Deckers, J., Gebrehiwot, K., 2013. Application of a spatially distributed water balance model for
752 assessing surface water and groundwater resources in the Geba basin, Tigray, Ethiopia. *J. Hydrol.*
753 499, 110–123. <https://doi.org/http://dx.doi.org/10.1016/j.jhydrol.2013.06.026>
- 754 Graf, R., Przybyłek, J., 2018. Application of the WetSpa simulation model for determining conditions
755 governing the recharge of shallow groundwater in the Poznań Upland, Poland. *Geologos* 24, 189–
756 205. <https://doi.org/10.2478/logos-2018-0020>
- 757 Guan, H., Love, A.J., Simmons, C.T., Hutson, J., Ding, Z., 2010. Catchment conceptualisation for
758 examining applicability of chloride mass balance method in an area with historical forest clearance.
759 *Hydrol. Earth Syst. Sci.* 14, 1233–1245. <https://doi.org/10.5194/hess-14-1233-2010>
- 760 Healy, R.W., Cook, P.G., 2002. Using groundwater levels to estimate recharge. *Hydrogeol. J.* 10, 91–109.
- 761 Hornero, J., Manzano, M., Ortega, L., Custodio, E., 2016. Environment Integrating soil water and tracer
762 balances , numerical modelling and GIS tools to estimate regional groundwater recharge :
763 Application to the Alcadozo Aquifer System (SE Spain). *Sci. Total Environ.* 568, 415–432.
764 <https://doi.org/10.1016/j.scitotenv.2016.06.011>
- 765 Hurni, H., Tato, K., Zeleke, G., 2005. The Implications of Changes in Population, Land Use, and Land
766 Management for Surface Runoff in the Upper Nile Basin Area of Ethiopia. *Mt. Res. Dev.* 25, 147–
767 154. [https://doi.org/10.1659/0276-4741\(2005\)025\[0147:TIOCIP\]2.0.CO;2](https://doi.org/10.1659/0276-4741(2005)025[0147:TIOCIP]2.0.CO;2)
- 768 Jepsen, D.H., Athearn, M.J., 1961. A general Geologic map of the Blue Nile River Basin, Ethiopia (1: 1,
769 000, 000), Department of Water Resources, Addis Ababa.
- 770 Johnson, A.I., 1967. Specific yield: compilation of specific yields for various materials. US Gov. Print.
771 Off.
- 772 Kebede, S., Travi, Y., Alemayehu, T., Ayenew, T., 2005. Groundwater recharge, circulation and
773 geochemical evolution in the source region of the Blue Nile River, Ethiopia. *Appl. Geochemistry*
774 20, 1658–1676. <https://doi.org/10.1016/j.apgeochem.2005.04.016>
- 775 Kebede, S., Travi, Y., Alemayehu, T., Marc, V., 2006. Water balance of Lake Tana and its sensitivity to
776 fluctuations in rainfall, Blue Nile basin, Ethiopia. *J. Hydrol.* 316, 233–247.
777 <https://doi.org/10.1016/j.jhydrol.2005.05.011>
- 778 Mamo, S., 2015. Integrated Hydrological and Hydrogeological System Analysis of the Lake Tana Basin,
779 Northwestern Ethiopia. PhD Thesis, Addis Ababa, Ethiopia.



- 780 Manna, F., Cherry, J.A., Mcwhorter, D.B., Parker, B.L., 2016. Groundwater recharge assessment in an
781 upland sandstone aquifer of southern California. *J. Hydrol.* 541, 787–799.
782 <https://doi.org/10.1016/j.jhydrol.2016.07.039>
- 783 Marechal, J.C., Dewandel, B., Ahmed, S., Galeazzi, L., Zaidi, F.K., 2006. Combined estimation of
784 specific yield and natural recharge in a semi-arid groundwater basin with irrigated agriculture. *J.*
785 *Hydrol.* 329, 281–293. <https://doi.org/10.1016/j.jhydrol.2006.02.022>
- 786 Minucci, E., 1938. Ricerche geologiche nella regione del Tana. Missione di Studio al Lago Tana. R.
787 *Accad. Ital* 1, 19–36.
- 788 Moon, S.K., Woo, N.C., Lee, K.S., 2004. Statistical analysis of hydrographs and water-table fluctuation
789 to estimate groundwater recharge. *J. Hydrol.* 292, 198–209.
790 <https://doi.org/10.1016/j.jhydrol.2003.12.030>
- 791 Nigate, F., 2019. Investigating the hydrogeological system of the Lake Tana basin in the northwestern
792 highlands of Ethiopia (the Upper Blue Nile). *Gelogy Department, Ghent University, Belgium.*
- 793 Nigate, F., Camp, M. Van, Yenehun, A., Belay, A.S., Walravaens, K., 2020. Recharge – Discharge
794 Relations of Groundwater in Volcanic Terrain of Semi-Humid Tropical Highlands of Ethiopia : The
795 Case of Infranz Springs , in the Upper. *Water* 12, 1–18.
- 796 Obuobie, E., Diekkrueger, B., Agyekum, W., Agodzo, S., 2012. Groundwater level monitoring and
797 recharge estimation in the White Volta River basin of Ghana. *J. African Earth Sci.* 71–72, 80–86.
798 <https://doi.org/10.1016/j.jafrearsci.2012.06.005>
- 799 Paola, G.M.D.I., 1972. The Ethiopian Rift Valley (Between 7 ° Off and 8 ° 40 ' lat . North). *Bull.*
800 *Volcanol.* 36, 517–560.
- 801 Rientjes, T.H.M., Perera, B.U.J., Haile, A.T., Reggiani, P., Muthuwatta, L.P., 2011. Regionalisation for
802 lake level simulation - The case of Lake Tana in the Upper Blue Nile, Ethiopia. *Hydrol. Earth Syst.*
803 *Sci.* 15, 1167–1183. <https://doi.org/10.5194/hess-15-1167-2011>
- 804 Scanlon, B.R., Healy, R.W., Cook, P.G., 2002. Choosing appropriate techniques for quantifying
805 groundwater recharge. *Hydrogeol. J.* 10, 18–39.
- 806 Setegn, S., Srinivasan, R., Dargahi, B., 2008. Hydrological Modelling in the Lake Tana Basin, Ethiopia
807 Using SWAT Model. *Open Hydrol. J.* 2, 49–62.
- 808 SMEC, 2008. Hydrological Study of the Tana-Beles Sub-basins: Surface Water Investigations. Addis



- 809 Ababa, Ethiopia.
- 810 Somaratne, N., Smettem, K.R.J., 2014. Theory of the generalized chloride mass balance method for
811 recharge estimation in groundwater basins characterised by point and diffuse recharge. *Hydrol.*
812 *Earth Syst. Sci. Discuss.* 11, 307–332. <https://doi.org/10.5194/hessd-11-307-2014>
- 813 Tekleab, S., Uhlenbrook, S., Mohamed, Y., Savenije, H.H.G., Temesgen, M., Wenninger, J., 2011. Water
814 balance modeling of Upper Blue Nile catchments using a top-down approach. *Hydrol. Earth Syst.*
815 *Sci.* 15, 2179–2193. <https://doi.org/10.5194/hess-15-2179-2011>
- 816 Tesemma, Z.K., Mohamed, Y.A., Steenhuis, T.S., 2010. Trends in rainfall and runoff in the Blue Nile
817 Basin : 1964 – 2003. *Hydrol. Process.* 24, 3747–3758. <https://doi.org/10.1002/hyp.7893>
- 818 Tilahun, K., Merkel, B.J., 2009. Estimation of groundwater recharge using a GIS-based distributed water
819 balance model in Dire Dawa, Ethiopia. *Hydrogeol. J.* 17, 1443–1457.
820 <https://doi.org/10.1007/s10040-009-0455-x>
- 821 Uugulu, S., Wanke, H., 2020. Estimation of groundwater recharge in savannah aquifers along a
822 precipitation gradient using chloride mass balance method and environmental isotopes, Namibia.
823 *Phys. Chem. Earth* 116, 102844. <https://doi.org/10.1016/j.pce.2020.102844>
- 824 Wale, A., Rientjes, T.H.M., Gieske, A.S.M., Getachew, H.A., 2009. Ungauged catchment contributions to
825 Lake Tana ' s water 3693, 3682–3693. <https://doi.org/10.1002/hyp>
- 826 Walker, D., Parkin, G., Schmitter, P., Gowing, J., Tilahun, S.A., Haile, A.T., Yimam, A.Y., 2019.
827 Insights From a Multi-Method Recharge Estimation Comparison Study. *Groundwater* 57, 245–258.
828 <https://doi.org/10.1111/gwat.12801>
- 829 Woldesenbet, T.A., Elagib, N.A., Ribbe, L., Heinrich, J., 2017. Hydrological responses to land use/cover
830 changes in the source region of the Upper Blue Nile Basin, Ethiopia. *Sci. Total Environ.* 575, 724–
831 741. <https://doi.org/10.1016/j.scitotenv.2016.09.124>
- 832 Yenehun, A., Nigate, F., Belay, A.S., Desta, M.T., Van Camp, M., Walraevens, K., 2020. Groundwater
833 recharge and water table response to changing conditions for aquifers at different physiography: The
834 case of a semi-humid river catchment, northwestern highlands of Ethiopia. *Sci. Total Environ.* 748,
835 142243. <https://doi.org/10.1016/j.scitotenv.2020.142243>
- 836 Zhu, R., Croke, B.F.W., Jakeman, A.J., 2020. Diffuse groundwater recharge estimation confronting
837 hydrological modelling uncertainty. *J. Hydrol.* 584, 124642.
838 <https://doi.org/10.1016/j.jhydrol.2020.124642>